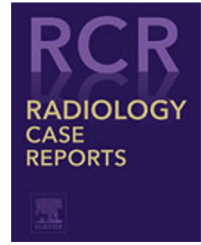


Available online at www.sciencedirect.com

ScienceDirect

journal homepage: www.elsevier.com/locate/radcr

Case Report

Cerebral proliferative angiopathy depicted by four-dimensional computed tomographic angiography: A case report[☆]

Shuichi Ito, MD^{a,#,*}, Mitsunori Kanagaki, MD, PhD^a, Naoya Yoshimoto, MD^b, Yoichiro Hijikata, MD^a, Marina Shimizu, MD^c, Hiroyuki Kimura, MD, PhD^a

^a Department of Diagnostic Radiology, Hyogo Prefectural Amagasaki General Medical Center, Hyogo, Japan

^b Department of Neurosurgery, Hyogo Prefectural Amagasaki General Medical Center, Hyogo, Japan

^c Department of Diagnostic Radiology, Japanese Red Cross Wakayama Medical Center, Wakayama, Japan

ARTICLE INFO

Article history:

Received 2 March 2022

Accepted 30 March 2022

Keywords:

Cerebral proliferative angiopathy

4D-CTA

Four-dimensional computed

tomographic angiography

Time-resolved CT angiography

DSA

Digital subtraction angiography

ABSTRACT

Cerebral proliferative angiopathy is a rare cerebrovascular disorder characterized by diffuse abnormal vessels with intermingled brain parenchyma fed by many arteries and draining into many veins without high-flow arteriovenous shunts, which is usually confirmed by conventional digital subtraction angiography. However, dilution of the contrast medium due to the markedly increased blood flow and volume in cerebral proliferative angiopathy leads to low-contrast angiography. We report a 53-year-old man with cerebral proliferative angiopathy who underwent CT, MR imaging, MR angiography, digital subtraction angiography and 4D-CTA. The 4D-CTA exhibited abnormal vessels without early venous filling between the atrophic brain parenchyma in higher contrast than the angiography due to high spatial and time resolution, whereas the left external carotid angiography visualized the characteristic transdural supply more clearly than the 4D-CTA due to high vascular selectivity. Therefore, novel 4D-CTA and conventional angiography plays a complementary role in the accurate diagnosis of cerebral proliferative angiopathy. Taking invasiveness into account, 4D-CTA may be advantageous for the diagnosis of cerebral proliferative angiopathy based on the characteristic imaging findings.

© 2022 The Authors. Published by Elsevier Inc. on behalf of University of Washington.

This is an open access article under the CC BY-NC-ND license

(<http://creativecommons.org/licenses/by-nc-nd/4.0/>)

[☆] Competing Interests: The authors declare no conflicts of interest associated with this manuscript.

* Corresponding author

E-mail address: pk.shuichi.ito@gmail.com (S. Ito).

Present and/or permanent address: Higashinaniwa-cho 2-17-77, Amagasaki City, 660-8550, Hyogo, Japan

<https://doi.org/10.1016/j.radcr.2022.03.104>

1930-0433/© 2022 The Authors. Published by Elsevier Inc. on behalf of University of Washington. This is an open access article under the CC BY-NC-ND license (<http://creativecommons.org/licenses/by-nc-nd/4.0/>)

Introduction

Cerebral proliferative angiopathy (CPA) is a rare cerebrovascular disorder characterized by diffuse abnormal vessels with intermingled brain parenchyma fed by many arteries and draining into many veins without high-flow arteriovenous shunts, which is distinct from cerebral arteriovenous malformation (AVM) and arteriovenous fistula (AVF) [1–5]. CPA is usually confirmed by conventional digital subtraction angiography (DSA). However, dilution of the contrast medium due to the markedly increased blood flow and volume in CPA often leads to low-contrast DSA. Although imaging findings and usefulness of 4D-CTA have been reported in cerebrovascular disorders including AVM and AVF [6–10], imaging findings in CPA are limited. We report a case of CPA with novel imaging findings on 4D-CTA and demonstrate the advantages of 4D-CTA for the diagnosis of CPA.

Case report

A 53-year-old man was admitted to our hospital with left-sided weakness for 2 months. His laboratory findings, medical history and family history were not significant. He did not have other symptoms, including headache and seizure, or body surface abnormalities, including facial hemangioma. Unenhanced and contrast-enhanced CT (CECT) revealed brain atrophy of the right hemisphere, especially the frontal lobe, with subcortical spotty calcification (Fig. 1A, arrow) and diffuse abnormal vessels (Figs. 1B, C, and D). On MR imaging and MR angiography (MRA), the abnormal vessels were observed between the atrophic brain parenchyma, which mainly divided into arterial components and venous components (Fig 1E-L). The arterial components were fed by the right anterior cerebral artery (ACA), right middle cerebral artery (MCA) and right posterior cerebral artery (PCA), with strong flow signal on MRA (Figs. 1K and L). The venous components were draining into cortical veins and into deep venous systems, including the great vein of Galen with slightly strong flow signal on MRA (Fig. 1K and L). Based on the CT and MR imaging findings, diffuse arteriovenous shunts, such as AVM and diffuse pial/dural AVF, were considered as differential diagnoses. On digital subtraction angiography (DSA), the abnormal vessels were fed by the right ACA, right MCA, and right PCA without early venous filling (Figs. 2A-C). In addition, on left external carotid angiography, characteristic transdural supply was observed (Fig. 3B, arrowhead). However, dilution of the contrast medium due to the markedly increased blood flow and volume led to low-contrast right internal carotid angiography despite power injection (Figs. 2A-C). Therefore, 4D-CTA was performed using an Aquilion ONE/ViSION edition multidetector CT scanner (Canon Medical Systems) equipped with 320 × 0.5 mm detector rows covering 16 cm of volume per rotation. Imaging was performed in the same manner as previously described [6–10]. On 4D-CTA, the abnormal vessels were visualized in high contrast, demonstrating no early venous filling in any phase of the 0.5-second time interval (Figs. 2D-F and Figs. 3D-F). Transdural supply from the left external

carotid artery was also observed (Fig. 3E, arrowhead). Perfusion images generated on 4D-CTA revealed increased cerebral blood flow (CBF, Fig. 4A) and cerebral blood volume (CBV, Fig. 4B), and a slightly decreased time to peak (TTP, Fig. 4C) and mean transit time (MTT, Fig. 4D) in the lesion. Based on these imaging findings, unlike AVM and AVF, the abnormal vessels had no high-flow arteriovenous shunts, and the patient was finally diagnosed with CPA in accordance with the previously reported imaging findings [1–5]. His symptoms and imaging findings remained unchanged 1 year after the diagnosis.

Discussion

We report novel imaging findings of CPA on 4D-CTA. Similar to the previously reported 4D-CTA of AVM and AVF [6–10], 4D-CTA of CPA visualized the hemodynamics as well as DSA. Moreover, 4D-CTA exhibited the abnormal vessels in higher contrast than right internal carotid angiography due to high spatial and time resolution, whereas the left external carotid angiography visualized the transdural supply, which is one of the characteristic findings of CPA [1,3–5], more clearly than 4D-CTA due to high vascular selectivity. Therefore, the high contrast of 4D-CTA and the high vascular selectivity of DSA play complementary roles in assessing the hemodynamics of CPA. In addition, 4D-CTA is less invasive than DSA. The examination processes of 4D-CTA include intravenous infusion of the contrast medium, whereas those of DSA include catheter insertion, intra-arterial administration of the contrast medium and perioperative patient care. Moreover, the examination time of 4D-CTA is shorter than that of DSA. In terms of radiation exposure, the CTDIvol of 463.6 mGy for 4D-CTA was lower than the calculated total radiation exposure of 892.3 mGy for DSA in this case. Taking invasiveness into account, 4D-CTA may be advantageous for the diagnosis of CPA based on the characteristic imaging findings.

Perfusion images generated on 4D-CTA demonstrated increased CBF and CBV, and a slightly decreased TTP and MTT in the lesion. These findings suggested that a large amount of blood passes through the abnormal vessels relatively quickly, which is consistent with dilution of the contrast medium due to the markedly increased blood flow and volume on DSA. Increased CBF and CBV are similar to the previously reported findings on MR perfusion imaging, whereas slightly decreased TTP and MTT are not [1,4,11–14]. Moreover, acetazolamide-stressed *N*-isopropyl-*p*-[¹²³I] iodoamphetamine single-photon emission computed tomography (¹²³I-IMP-SPECT) demonstrated decreased CBF and cerebrovascular reactivity [3,4,13,15–17], and ^{99m}Tc-ethylcysteinate dimer single-photon emission computed tomography (^{99m}Tc-ECD-SPECT) [4,18] suggested hypoperfusion over the affected brain parenchyma. Reported findings on ¹⁸F-fluorodeoxyglucose positron emission tomography (¹⁸F-FDG-PET) included hypometabolism in the lesion [4,19]. These discrepancies mainly result from the perfusion images generated by 4D-CTA reflecting the abnormal vessels themselves, not the brain parenchyma, although the permeability of the tracer, the degree of disease progression, impaired blood brain barrier,

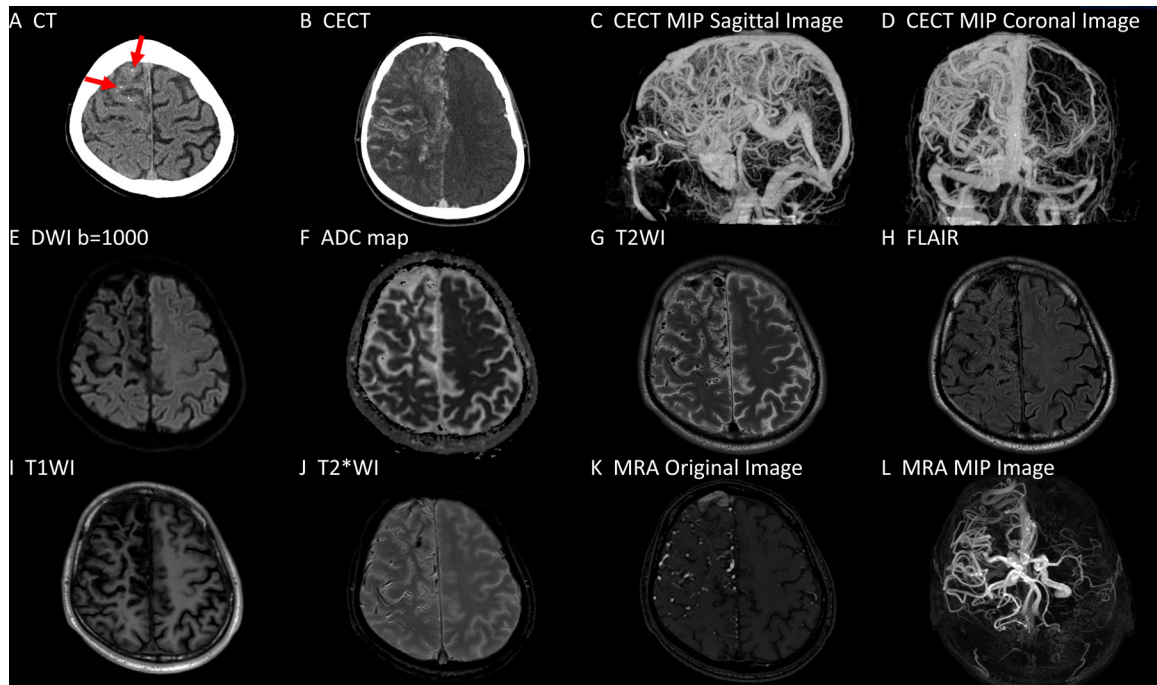


Fig. 1 – On CT, the right hemisphere, especially the frontal lobe, exhibited atrophy with subcortical spotty calcification (A, arrow). On contrast-enhanced CT (CECT), abnormal vessels were enhanced (B). The maximum intensity projection (MIP) images revealed the overall picture of the abnormal vessels, which consisted of many arteries and veins (C and D). On MR imaging, atrophic brain parenchyma was observed between the abnormal vessels (G–K). The affected right hemisphere did not show restricted diffusion (E and F) or hemorrhagic change (J). On MR angiography (MRA), the arterial component of the abnormal vessels showed strong flow signal and venous component of the abnormal vessels exhibited slightly strong flow signals (K and L).

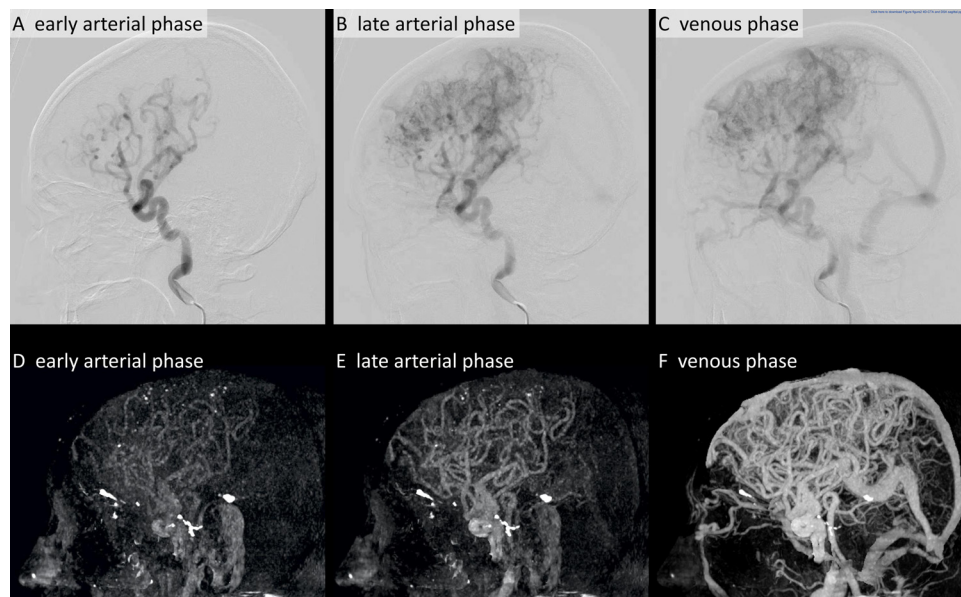


Fig. 2 – On right internal carotid angiography, abnormal vessels were observed without early venous filling (A, B, and C). Due to a markedly increased blood flow and volume, right internal carotid angiography had lower contrast than 4D-CTA despite power injection. On 4D-CTA, the abnormal vessels were visualized in higher contrast than on right internal carotid angiography (D, E, and F).

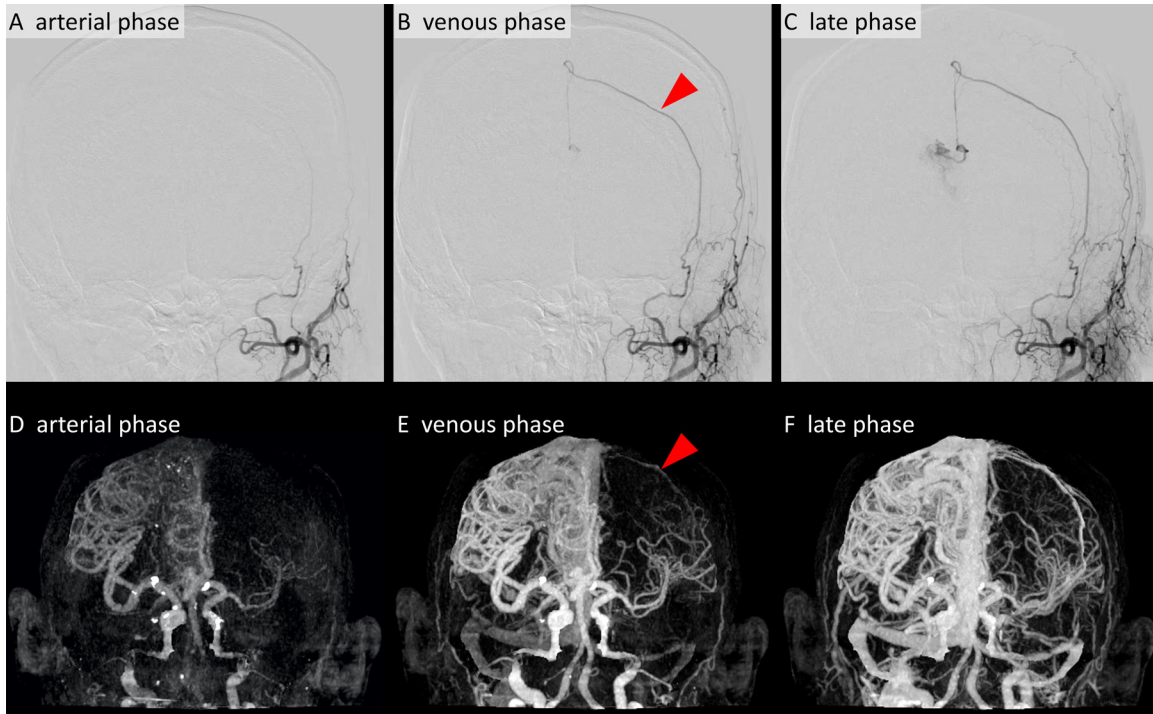


Fig. 3 – On left external carotid angiography, characteristic transdural supply was observed (B, arrowhead). On 4D-CTA, transdural supply was also observed (E, arrowhead). Left external carotid angiography more clearly visualized the transdural supply than 4D-CTA.

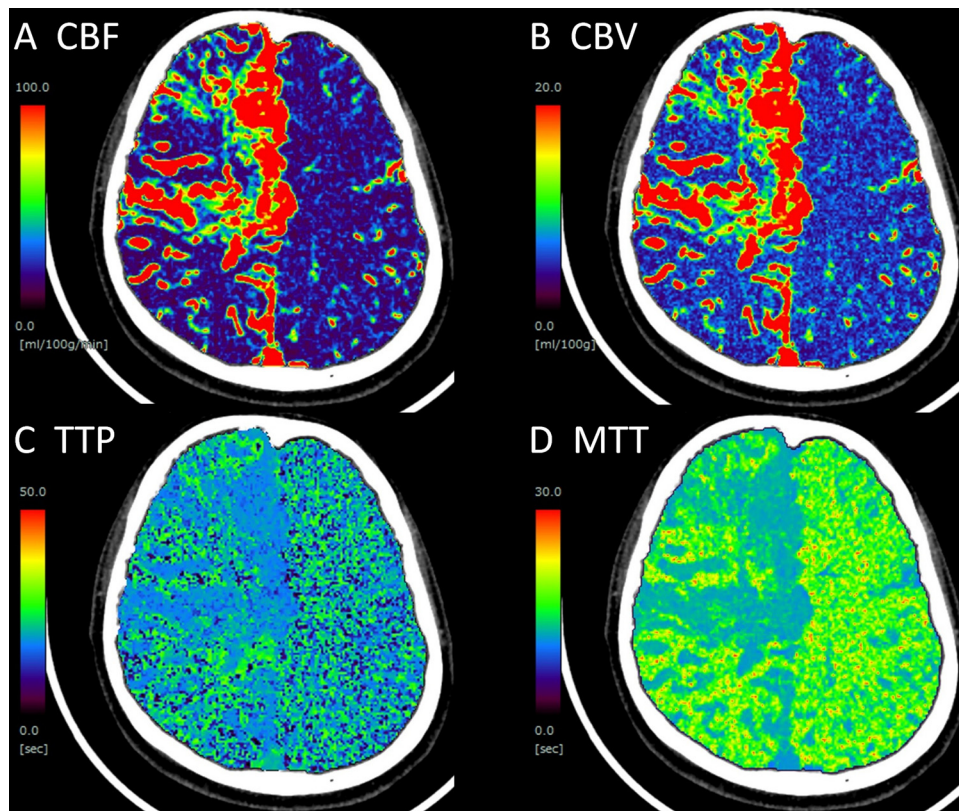


Fig. 4 – Perfusion images generated by 4D-CTA showed increased cerebral blood flow (CBF, A) and cerebral blood volume (CBV, B), and slightly decreased time to peak (TTP, C) and mean transit time (MTT, D) in the lesion. These findings suggested that a large amount of blood passed through the abnormal vessels relatively quickly.

and treatment are also considered candidate causes. The calculated apparent blood perfusion increased on 4D-CTA, but the net amount of blood perfusing the brain parenchyma is considered to be lower.

In summary, we reported imaging findings, including those on 4D-CTA, in a rare case of CPA. The utility of 4D-CTA in the diagnosis of CPA was demonstrated. The higher contrast and lower invasiveness of 4D-CTA will facilitate the accurate diagnosis of CPA.

Patient consent

Written and informed consent was received from the patient.

REFERENCES

- [1] Lasjaunias PL, Landrieu P, Rodesch G, Alvarez H, Ozanne A, Holmin S, et al. Cerebral proliferative angiopathy: clinical and angiographic description of an entity different from cerebral AVMs. *Stroke* 2008;39(3):878–85. doi:10.1161/STROKEAHA.107.493080.
- [2] Geibprasert S, Pongpech S, Jiarakongmun P, Shroff MM, Armstrong DC, Krings T. Radiologic assessment of brain arteriovenous malformations: what clinicians need to know. *Radiographics* 2010;30(2):483–501. doi:10.1148/rg.302095728.
- [3] Liu P, Lv X, Lv M, Li Y. Cerebral proliferative angiopathy: clinical, angiographic features and literature review. *Interv Neuroradiol* 2016;22(1):101–7. doi:10.1177/1591019915609784.
- [4] Somji M, McEachern J, Silvaggio J. Cerebral revascularization in cerebral proliferative angiopathy: a systematic review. *Neurosurg Focus* 2019;46(2):E11. doi:10.3171/2018.11.FOCUS18529.
- [5] Yamaki VN, Solla DJF, Telles JPM, Liem GLJ, Silva SA, Caldas JGMP, et al. The current clinical picture of cerebral proliferative angiopathy: systematic review. *Acta Neurochir (Wien)* 2020;162(7):1727–33. doi:10.1007/s00701-020-04289-7.
- [6] Brouwer PA, Bosman T, van Walderveen MAA, Krings T, Leroux AA, Willems PWA. Dynamic 320-section CT angiography in cranial arteriovenous shunting lesions. *AJNR Am J Neuroradiol* 2010;31(4):767–70. doi:10.3174/ajnr.A1747.
- [7] Willems PWA, Brouwer PA, Barfett JJ, terBrugge KG, Krings T. Detection and classification of cranial dural arteriovenous fistulas using 4D-CT angiography: initial experience. *AJNR Am J Neuroradiol* 2011;32(1):49–53. doi:10.3174/ajnr.A2248.
- [8] Willems PWA, Taeshineetanakul P, Schenk B, Brouwer PA, terBrugge KG, Krings T. The use of 4D-CTA in the diagnostic work-up of brain arteriovenous malformations. *Neuroradiology* 2012;54(2):123–31. doi:10.1007/s00234-011-0864-0.
- [9] Kortman HGJ, Smit EJ, Oei MTH, Manniesing R, Prokop M, Meijer FJA. 4D-CTA in neurovascular disease: a review. *AJNR Am J Neuroradiol* 2015;36(6):1026–33. doi:10.3174/ajnr.A4162.
- [10] Veld MI, Fronczek R, dos Santos MP, van Walderveen MAA, Meijer FJA, Willems PWA. High sensitivity and specificity of 4D-CTA in the detection of cranial arteriovenous shunts. *Eur Radiol* 2019;29(11):5961–70. doi:10.1007/s00330-019-06234-4.
- [11] Ducreux D, Petit-Lacour MC, Marsot-Dupuch K, Bittoun J, Lasjaunias P. MR perfusion imaging in a case of cerebral proliferative angiopathy. *Eur Radiol* 2002;12(11):2717–22. doi:10.1007/s00330-001-1293-y.
- [12] Vargas MC, Castillo M. Magnetic resonance perfusion imaging in proliferative cerebral angiopathy. *J Comput Assist Tomogr* 2011;35(1):33–8. doi:10.1097/RCT.0b013e3181ff1e79.
- [13] Kimiwada T, Hayashi T, Takahashi M, Shirane R, Tominaga T. ¹²³I-IMP-SPECT in a patient with cerebral proliferative angiopathy: a case report. *J Stroke Cerebrovasc Dis* 2013;22(8):1432–5. doi:10.1016/j.jstrokecerebrovasdis.2013.05.038.
- [14] Tiwari S, Garg PK, Khera PS, Babu S, Sureka B, Yadav T. Cerebral proliferative angiopathy: an uncommon and misdiagnosed entity. *J Clin Interv Radiol ISVIR* 2020;4:107–10. doi:10.1055/s-0039-3401329.
- [15] Fukui I, Uchiyama N, Mouri M, Misaki K, Aida Y, Nambu I. Management of cerebral proliferative angiopathy with indirect revascularization: a case report. *Surg Cereb Stroke (Jpn)* 2015;43:335–7.
- [16] Sakata H, Fujimura M, Sato K, Niizuma K, Endo H, Tominaga T. Development of abnormal hemispheric vascular networks mimicking cerebral proliferative angiopathy in a child originally diagnosed with deep-seated arteriovenous fistula. *J Stroke Cerebrovasc Dis* 2016;25(10):e200–4. doi:10.1016/j.jstrokecerebrovasdis.2016.07.042.
- [17] Kimiwada T, Hayashi T, Takahashi M, Shirane R, Tominaga T. Progressive cerebral ischemia and intracerebral hemorrhage after indirect revascularization for a patient with cerebral proliferative angiopathy. *J Stroke Cerebrovasc Dis* 2019;28(4):853–8. doi:10.1016/j.jstrokecerebrovasdis.2018.11.021.
- [18] Kono K, Terada T. Encephaloduroarteriosynangiosis for cerebral proliferative angiopathy with cerebral ischemia. *J Neurosurg* 2014;121(6):1411–15. doi:10.3171/2014.7.JNS132793.
- [19] Kolderman SEM, Noordzij W, van Dijk JMC, Luijckx GJR. Nuclear imaging in proliferative angiopathy. *Eur J Nucl Med Mol Imaging* 2014;41(4):810. doi:10.1007/s00259-013-2645-y.